COMMUNICATIONS IN COMPUTATIONAL PHYSICS
Vol. **6**, No. 1, pp. 24-48

Commun. Comput. Phys.
July 2009

Constructing Three-Phase Capillary Pressure Functions by Parameter Matching Using a Modified Ensemble Kalman Filter

Randi Holm*, Roland Kaufmann, Elisabeth Iren Dale, Sigurd Aanonsen, Gunnar E. Fladmark, Magne Espedal and Arne Skauge

Centre for Integrated Petroleum Research / University of Bergen, P.O. Box 7800, 5020 Bergen, Norway.

Received 11 November 2007; Accepted (in revised version) 15 July 2008

Available online 13 November 2008

Abstract. Usually extended two-phase capillary pressures are used in three-phase simulations, because three-phase capillary pressures are not possible or hard to measure. In this work three-phase capillary pressure surfaces are created by at pore network model. The input parameters to this network model are found by matching two-phase capillary pressure curves. This matching is done with a slightly modified EnKF routine. Tables with three-phase capillary pressures are created and used as input to flow simulations.

AMS subject classifications: 76T30, 37M05, 37N10, 35Q80, 60G35, 62M20, 62F15, 45Q05

Key words: Ensemble Kalman Filter (EnKF), three-phase porous media flow, capillary pressure, parameter matching.

1 Introduction

When starting production from an oil reservoir the pressure drops, and this pressure needs to be replaced if you want high oil recovery. Injection of water is the most common way to maintain the pressure, but also injection of gas is used.

In recent years it has been shown that a water-alternating-gas (WAG) scenario, where short slugs of gas and water are injected in a sequence, results in lower residual oil, less trapped oil in the reservoir, than if you inject only water or only gas. Skauge and Stensen reported an increased oil recovery from WAG of five to ten percent of the initial oil in place [1].

*Corresponding author. *Email addresses:* Randi.Holm@math.uib.no (R. Holm), Roland.Kaufmann@cipr.uib.no (R. Kaufmann), elid@statoilhydro.com (E. I. Dale), Sigurd.Aanonsen@cipr.uib.no (S. Aanonsen), Gunnar.Fladmark@cipr.uib.no (G. E. Fladmark), Magne.Espedal@math.uib.no (M. Espedal), Arne.Skauge@cipr.uib.no (A. Skauge)

The combination of gas and water gives many favorable effects [2, 3]. Gas results in better microscopic displacement; less oil left in the pores of the gas swept areas when compared to water swept areas. The zones swept with both gas and water may have even lower trapped oil saturation [4–7].

The water is controlling the mobility of gas and consequently the stability of the displacement front i.e. the transition zone between injected fluid and oil. The result is better macroscopic displacement of the oil. Without water present the gas would sweep a much smaller volume, because the gas would then zoom through at the top of the reservoir or through zones with high pore connectivity, high permeability. There would be more oil left in the reservoir and earlier breakthrough of gas in the producers.

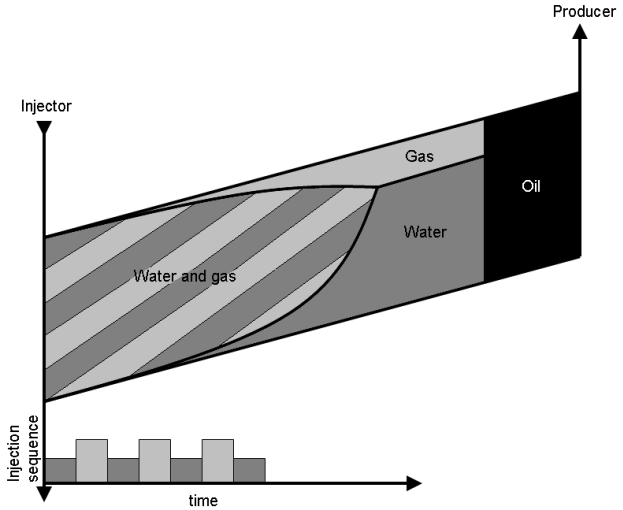

Figure 1: Schematic sketch of WAG injection (Adapted from NPD [5]).

In thick homogeneous reservoirs the main advantage of WAG is the improved vertical sweep due to gravity segregation of water and gas. The water sinks to the bottom and the gas rises to the top of the reservoir. This effect can be seen in Fig. 1. At the top of the reservoir we get two-phase flow of gas and oil, and near the bottom we get two-phase flow of water and oil. In parts of the reservoir, especially close to the injector we get three-phase flow of gas, water and oil. Gas, water and oil are then flowing simultaneously and interacting in the reservoir.

In homogeneous reservoirs the gas and water may segregate rapidly and the three-phase zone is then located close to the injector. The region with three-phase flow can in many cases extend to a considerable part of the reservoir. More heterogeneous reservoirs may have a slower segregation of the fluids. Lower mobility of gas and water in the three-phase zone also delays the segregation process [6, 7].

The influence of capillary pressure is often neglected in complex three-phase processes like immiscible WAG. There is very little experimental data on three phase capillary pressure available. In Kalaydjian [8], three-phase capillary pressure was measured

for both drainage and imbibition on an outcrop water-wet core and on unconsolidated material. The experimental data show the complexity of three-phase capillary pressure as both drainage and imbibition capillary pressures were found to depend on more than one phase saturations. The three-phase capillary pressure was higher than the corresponding two-phase capillary pressure.

More recently there has been several attempts to estimate three-phase capillary pressure from network modeling [9–11]. Among the results is the fact that the gas/water capillary pressure curves depend strongly on the spreading coefficient and the oil/water capillary pressure [9]. The trend in capillary pressure variation from two-phase to three-phase situations is similar in the network derived capillary pressure [11] as in the data from Kalaydjian [8]. The network data has been generated by anchoring the network to drainage and imbibition two-phase capillary pressure. Thereafter the three-phase capillary pressure (Pc) was estimated on the conditioned network representing pore size distribution and wetting properties.

Although the experimental data is very limited, there already exist developed correlations for three-phase capillary pressure [12]. These types of analytical functions are in particular useful and needed when generating input data to reservoir simulations.

The article will be organized in the following way: Subsection 1.1 will describe the work flow and explain the mathematical model for the needed three-phase parameters. Section 2 is a discussion of possible approaches to solve the inverse problem, and Section 3 introduces stochastic filters and explains the adapted Ensemble Kalman filter. In Section 4 we have used this filter to find estimates for the parameters by anchoring three-phase capillary pressures to two-phase capillary pressure curves. The parameters are used to construct three-phase capillary pressure functions, as explained in Section 5. Conclusions and further work are summarized in Section 6. The nomenclature used to explain the adapted Ensemble Kalman filter is listed in Appendix A. Parameters from the network model are explained in Appendix B.

1.1 Mathematical model and work flow

WAG injection is becoming more common and the need for describing the WAG dynamics consequently becomes more important. Immiscible WAG injection includes complex multi-phase, multi-component flow problems. On a continuous macro scale, the WAG flow is described mathematically by a three-phase, three component model (Black Oil model) [13, 14]. The alternation of injection fluids leads to strong hysteresis effects. Earlier studies, including three-phase relative permeability hysteresis models have shown that the three-phase zone may extend to a large part of the reservoir [1, 4, 15]. The effect of capillarity has in earlier studies been neglected, and current research focus is on the impact of capillary pressure on three-phase flow related to WAG processes. Since capillary forces are controlling the main dynamics on pore level, the capillary pressure is expected to be an important factor describing the three-phase flow in a porous heterogeneous media.

A mathematical model for three-phase fluid flow processes through porous media needs the representation of three-phase parameters.

The three-phase relative permeabilities for water (w), oil (o) and gas (g) are [16]:

$$\begin{aligned} &k_{r\varphi} = k_{r\varphi}(S_w, S_g), \quad \text{for } \varphi = w,o,g, \\ &S_w + S_o + S_g = 1, \end{aligned} \tag{1.1}$$

where S_w, S_o and S_g are the water, oil and gas saturations.

Further the three-phase oil-water and gas-oil capillary pressures are given by:

$$Pc_{ow}(S_w, S_g) = p_o - p_w, \tag{1.2}$$

$$Pc_{go}(S_w, S_g) = p_g - p_o. \tag{1.3}$$

We note that all these three-phase parameters are given as surfaces in the (S_w, S_g)-space. Two-phase relative permeability and capillary pressures are functions of one saturation variable. The two-phase parameters can usually be measured experimentally, but the three-phase parameters are difficult or impossible to measure and must therefore be estimated by other methods [17]. The main objective of this work is to present a method to estimate three-phase capillary pressures.

A two-phase capillary pressure is defined in a saturation interval $[S_m, S_M]$, $S_m \geq 0$, $S_M \leq 1$, where S_m is the residual saturation of the non-wetting fluid and $1 - S_M$ is the irreducible saturation of the wetting fluid [13]. The capillary pressure curves may have an asymptotic behaviour at $S = S_m$ and $S = S_M$.

In this work we will use a three-phase network model to estimate the three-phase capillary pressures. The network simulator used is developed at the Heriot Watt University, Edinburgh [18]. It has different input parameters describing fluid properties, pore properties (geometry) and wettability properties. The main steps in our work flow to estimate the three-phase capillary pressures are:

- Get data from two-phase capillary pressure measurements and data for fluid properties from the literature.
- Anchor the input parameters in a network simulator by matching the data. This is done by using adapted Ensemble Kalman Filter (EnKF) method.
- Run the network simulator for systematic variations of the saturations as input to produce three-phase capillary pressures.

This approach is based on the assumption that the three-phase capillary pressures will go to the limit of a two-phase capillary pressure when the saturation of one of the phases goes to zero.

The details of the procedure will be presented in the following chapters. Similar consistent estimation methods for the three-phase relative permeabilities will be presented in later work.

2 Comments on using a classic, direct technique

Simulation of pore-scale flooding contains a vast amount of parameters that guide the process, and this presents some challenges to textbook anchoring methods.

To determine how close we are to a solution that matches our data, we need a way to quantify this. Usually, this is done by introducing an objective function which maps a solution to a target value, such that the objective function is decreasing when it gets closer to the true value. Fitting the parameters now becomes a question of minimizing this objective function.

Defining a good objective function is in itself not straightforward. The capillary pressure curves are assumed to behave according to a Brooks-Corey power-law function [22] which essentially capture three factors: (1) The entry pressure needed for flooding of the pores to start determines the horizontal asymptote, (2) connate water or residual oil saturation at which flooding is no longer possible determines the vertical asymptote, and (3) a measure of the pore-size distribution determines the speed at which flooding occurs, i.e., the bend of the curve.

Various parameters have different effect on each of these factors, and sets of parameters that give a good fit in one part of the curve may cause large deviation in another. An additional snag is that the capillary pressure tends towards infinity at the asymptotes, leading to problems in numerical representation.

First, we turn to the task of incorporating the output of the network simulator into a formulation that can be used in an objective function. Since a Brooks-Corey function is both continuous and has smooth derivatives, we settled in the preliminary evaluation for an orthogonal distance regression using a Levenberg-Marquardt algorithm [23] of the data points to a power-law function, and then use the integral between their inverses. Going through this extra hoop is necessary in order to make the output which may be at different locations comparable with the measurements. Even then, some choices must be made as to which pressure intervals should be considered. Selecting a larger interval will favour the asymptotes, whereas a smaller interval will favour the slope and position of the curve.

With an objective function defined, we next turned to the problem of minimizing it. This is not as easy as simply using the fitting procedure described above, since the objective function exhibits the characteristics of the network itself instead of that of the general behaviour.

Naïvely, the first thing to consider is to use brute force; to try out various combinations of parameters to see which one is best. The large number of dimensions in the problem makes this approach infeasible. Even if we just considered a low, medium and high value for each of the parameters, it would amount to evaluating 3^{40} combinations! Clearly, that is not going to work.

Another way of attacking the problem is to start out at some initial point and then use a scheme like a gradient method (see for instance [23,24]) to follow the target function to the minimum value.

However, pore-scale network simulations are done by modeling a discrete network of nodes and bonds, not by a discretization of a continuous field. Instead of computing an equation over all elements, a minimum displacement chain is located in the network for each transition from one steady state to another.

Altering the parameters may or may not have effect on the chains that are used, or only on some of them. For a small change, the network may take an entirely different path, or not be affected at all. There may be an effect on the aggregate of several realizations, but we cannot use the information from a single run alone.

Thus, the derivatives of the output with respect to the parameters tends to have threshold effects, where derivatives by numerical differentiation are very sensitive to the discretization. This may be countered by using several evaluations to approximate a gradient, but the computation of a single partial derivative then becomes very expensive.

Global methods, such as genetic algorithms or simulated annealing, may to some extent find global minimum of complex objective functions. However, such methods typically require thousands of simulation runs, which often is not feasible.

3 Ensemble Kalman Filter

Instead of using several network evaluations to do a deterministic search for a minimum, an alternative is to use the computer time to perform a statistical analysis of the behaviour.

The Ensemble Kalman Filter (EnKF) is a sequential data assimilation method which is designed for large-scale filtering problems [19–21, 25]. It is a Monte Carlo method where the probability distribution is represented by an ensemble of model realizations. Although it is based on a linearity assumption, it often works surprisingly well on problems with somewhat non-linear dynamics.

The method tries to minimize the mismatch between the measurements and the values computed by a simulator. The ensemble must be of a certain size to reduce sampling errors, but at some point, it will be better to average multiple filter runs rather than increasing the ensemble size [26].

The EnKF methodology consists of two steps; the forecast step and the assimilation step. In the forecast step the simulator is run forward for each of the ensemble members to the time of the next measurement. The assimilation step consists of updating the model variables by applying the Kalman equations on the output of these runs together with the measurements. In every time step one more measurement is matched, and the variation in the distribution of the parameters will hopefully decrease as the prior is combined with the likelihood calculated from this new information. Output from the method is then distributions of the input parameters to the simulator.

Some modifications had to be done before we could apply EnKF to our problem. Roughly said, what we have done is not to adjust the internal state of the model in each step but rather re-run the simulator from scratch with the new set of parameters. We also

introduce a sort of penalty term for results that are outside of the accepted domain.

A summary of the nomenclature used in the following paragraphs is provided in Appendix A.

As in the original EnKF algorithm we start out with a number of measurements $p_k^{(t)}$ for the capillary pressures. Here k is the measurement type for a total of q types. Informally, a measurement type is also known as a graph, since its measurements can be drawn as a such. We are trying to match three different types of measurements; the capillary pressure between gas and oil Pc_{go}, the capillary pressure between oil and water Pc_{ow} and the capillary pressure between mercury and nitrogen Pc_{hg}, so q is equal to three in our case. The number of measurements for each type is ω_k and $t\in[1,\omega_k]$ denotes the time step where the data point at saturation $s_k^{(t)}$ is matched.

Errors stem from two parts: Model errors and measurement errors. As we don't have any assumption about the model error, we have opted to assume that the model error is negligible and not attempted to quantify it nor bring it into the equations.

Comparable studies often report the error in a measurement to be within $\pm 10\%$ with 90% confidence. It is common to assume that the error follows a normal distribution, which means that there should be a standard deviation $\sigma_k^{(t)}$ of about 6% of the measured value for each type.[†]

Furthermore, we assume that errors made in different measurements are independent of each other, which gives us a diagonal covariance matrix E with elements:

$$e_{k,l}=\begin{cases}\sigma_k^2 & \text{if } k=l,\\ 0 & \text{otherwise,}\end{cases}\qquad \text{for } k,l\in[1,q]. \tag{3.1}$$

EnKF requires that we perturb the measurements across the ensemble to get a correct sampling [19–21]. This is done for each graph k by adding stochastic noise from the measurement distribution. That is, with n being the ensemble size:

$$d_{k,j}^{(t)}=p_k^{(t)}+\xi_{k,j}^{(t)},\quad \text{for } k\in[1,q],\ j\in[1,n], \tag{3.2}$$

where $\xi_{k,j}^{(t)}\sim\mathcal{N}(0,\sigma_k^{(t)})$ with new realizations for each timestep t. Perturbation must be done even if our measurements stem from a synthetic example generated by a deterministic model.

The network simulator takes m input parameters. Let $\boldsymbol{\alpha}$ be a vector of length m containing these parameters, and let $\boldsymbol{\alpha}^{(t)}$ be the most updated estimate at timestep t. Without much knowledge of the parameter space, we have chosen our a priori distributions to be uniformly distributed between their lower limits a_i and their upper limits b_i, where each parameter is indexed with $i\in[1,m]$.

EnKF is based on the assumption that the parameters are Gaussian, or approximately Gaussian, so we use the inverse normal cumulative distribution function g^{-1} — also

[†] $\frac{10\%}{-g^{-1}(\frac{1-90\%}{2})}\approx 6\%$, assuming tails on both sides

known as the quantile — to transform between uniformly distributed values to a set of values $\boldsymbol{\theta}$ in a Gaussian space with zero mean and unit standard deviation with elements:

$$\theta_i = g^{-1}\left(\frac{\alpha_i - a_i}{b_i - a_i}\right) \quad \text{for } i \in [1,m]. \tag{3.3}$$

Using Eq. (3.3), we can switch between actual parameters passed to the simulator and parameters used in the EnKF update equations. Since we go both ways, mapping in and out of the Gaussian space, the statistics of the filter does not change, but we get the effect of having a uniformly distributed prior assumption about the parameters.

Some of the parameters are maximum or minimum values for distributions. For instance, the radius for each pore in the network is internally drawn from a Rayleigh distribution, and the minimum and maximum pore-size for this distribution are input parameters to the simulator. If their intervals given by $[a_{min\_size}, b_{min\_size}]$ and $[a_{max\_size}, b_{max\_size}]$ overlap, it is possible that the minimum value drawn from the normal distribution corresponds to a value that is larger than the maximum value. This can also happen after an update of the filter. Such parameter values will not make sense in the network model, so this must be controlled for every time step. To fix it, both the maximum and the minimum values are set to the mean of the two:

$$\begin{aligned} \alpha'_{max\_size} &= \frac{\alpha_{max\_size} + \alpha_{min\_size}}{2}, \\ \alpha'_{min\_size} &= \frac{\alpha_{max\_size} + \alpha_{min\_size}}{2}, \end{aligned} \tag{3.4}$$

replacing $\alpha_{\{min,max\}\_size}$ with $\alpha'_{\{min,max\}\_size}$ if $\alpha_{max\_size} < \alpha_{min\_size}$.

By this procedure the parameters will change in the direction that the filter wants them to, but not so much that the maximum value becomes smaller than the minimum value.

The forward simulation is given by

$$\psi_k^{(t)} = f_k(\boldsymbol{\alpha}^{(t)}, s_k^{(t)}) \quad \text{for } k \in [1,q],\ t \in [1,\omega_k] \tag{3.5}$$

where f returns primarily capillary pressure ψ for each measurement type k when the simulator is run with the parameters $\boldsymbol{\alpha}$ towards a target saturation s for that timestep t.

However, the simulator is not always able to attain the desired saturation. In practice it only accepts certain saturation values, making this a partial function. This is due to the nature of the process, not the accuracy of the simulator, and is a problem at the beginning and in the end. The capillary pressure follows the behaviour of a power-law function which is limited by asymptotes (on one side for gas-oil, on both sides for oil-water). Outside of these asymptotes, the capillary pressure is not defined.

Let s_k^L be the saturation value for the left asymptote in graph k. That is, this is the first saturation value for which an output from the simulator could be obtained. Correspondingly, s_k^R is the saturation for the right asymptote.

At the asymptote, the capillary pressure curve is almost vertical and an insignificant change in saturation gives a huge change in pressure. Therefore, there is little meaning in comparing the pressures at this point. Instead, we compare the saturations for the asymptotes.

Simulations whose asymptotes are far apart from the goal will thus give results that indicate that those parameters are incorrect. To avoid preference for curves that starts earlier (or ends later), the condition is made symmetric to a distance on the other side of the asymptote as well.

This test is always done on the first measurement since that corresponds to the asymptote. Thereafter, the asymptote is checked at each timestep, but the pressure for that timestep is used if the asymptote is found to be acceptable.

Hence, we introduce a vector $\boldsymbol{y}$ of modified pressure values, with an element for each graph $k\in[1,q]$ given by:

$$y_k^{(t)}=\begin{cases} p_k^{(t)}+\min\left(2\frac{(s_k^{(1)}-s_k^{L(t)})}{\delta},6\right)\sigma_k^{(t)} & \text{if } t=1 \text{ or } |s_k^{(1)}-s_k^{L(t)}|>\delta, \text{ (left asymptote)},\\ p_k^{(t)}-\min\left(2\frac{(s_k^{(\omega_k)}-s_k^{R(t)})}{\delta},6\right)\sigma_k^{(t)} & \text{if } t=\omega_k \text{ or } |s_k^{(\omega_k)}-s_k^{R(t)}|>\delta, \text{ (right asymptote)},\\ \psi_k^{(t)} & \text{else}, \end{cases} \tag{3.6}$$

where $s_k^{(1)}$ is the measured asymptote and $s_k^{L(t)}$ is the simulated asymptote for the current parameter values.

It is advisable to choose a δ that is less than the distance between the saturations of two timesteps. Otherwise, one risks that the test does not trigger if a result is not defined for the second timestep either. (The first is always checked anyway). This value must be determined through some initial testing. We have used the value 0.05 for δ in this paper.

The EnKF is based on first running the forward model and then updating when new measurements become available. This is done for each ensemble member. Update is done with the standard Kalman filter update equations, combined with an ensemble approximation to the covariance matrices [20, 21]. Introducing the ensemble matrices Θ, Y and D holding the n ensemble members of $\boldsymbol{\theta}, \boldsymbol{y}$ and $\boldsymbol{d}$ in each column, the EnKF update equations may be written:

$$\Theta^{(t+1)}=\Theta^{(t)}+K^{(t)}\left(D^{(t)}-Y^{(t)}\right), \tag{3.7}$$

where $K^{(t)}$ is the Kalman gain matrix given by:

$$K^{(t)}=C_{\Theta Y}{}^{(t)}(C_{YY}{}^{(t)}+E^{(t)})^{-1}. \tag{3.8}$$

The covariances used above are given by the standard expressions:

$$C_{\Theta Y}=\frac{1}{n-1}(\Theta-\overline{\Theta})(Y-\overline{Y})^T,$$
$$C_{YY}=\frac{1}{n-1}(Y-\overline{Y})(Y-\overline{Y})^T,$$

where $\overline{Y}$ and $\overline{\Theta}$ are the matrices holding the ensemble means in each column:

$$\overline{\Theta} = \{\overline{\boldsymbol{\theta}}, \overline{\boldsymbol{\theta}}, \cdots \overline{\boldsymbol{\theta}}\} = \Theta \cdot \mathbf{1}_n, \tag{3.9a}$$

$$\overline{Y} = \{\overline{\boldsymbol{y}}, \overline{\boldsymbol{y}}, \cdots \overline{\boldsymbol{y}}\} = Y \cdot \mathbf{1}_n, \tag{3.9b}$$

where $\mathbf{1}_n$ is the n times n matrix with all elements equal to $1/n$.

Initial (prior) ensemble of parameters is set up by drawing i.i.d. values $\theta_{i,j}^{(1)} \sim \mathcal{N}(0,1)$.

If the residual is large, there will be large changes in the parameters. Exactly how large the changes will be is determined by the Kalman gain. If the distributions of parameters $\boldsymbol{\theta}$ and capillary pressures $\boldsymbol{y}$ are wide, the covariance matrix $C_{\Theta Y}$ will have large entries. If the entries in the matrices C_{YY} and E are large, this will have the opposite effect. E has large entries if we consider the uncertainties in the measurements to be large. The Kalman gain will therefore depend on the distributions of the parameters and the measurements.

The final solution parameters are taken as the mean of the last ensemble after update. The capillary pressure curve made by the network model with these parameters should match all the measurements according to the given standard deviation.

4 Anchoring capillary pressure curves to two-phase measurements

Measurements are developed in a laboratory with tests done at core plugs from a North Sea reservoir. The measurements are from injection of mercury into a core plug filled with nitrogen, injection of gas into a core plug filled with oil and residual water, and injection of water into a core plug filled with oil and residual water. From these experiments the capillary pressure between mercury and nitrogen, between gas and oil and between oil and water are used to determine the properties of the core plug. The experiments are done to different cores, but they are from the same area, such that their properties are assumed to be almost the same.

The injection of mercury and the injection of gas are both drainage processes, because a non-wetting phase is displacing a wetting phase. In a drainage process the injected fluid starts to go into the largest pores, where the capillary pressure needed to invade is the lowest. This capillary pressure is given by the Young-Laplace equation,

$$Pc = \frac{2\sigma\cos(\theta)}{r}, \tag{4.1}$$

where r is the radius of the pore, σ is the interfacial tension between the phases and θ is now the wetting angle between the phases. As smaller and smaller pores are filled, the capillary pressure needed to fill the next pore increases. The small pores decide how large the capillary pressure must be, such that drainage processes give an indication of the distribution of small pores. Similarly, in an imbibition process the injected fluid invades the smallest pores first, such that the distribution of the largest pores will be determined.

The input parameters to the network model can be categorised into three groups describing the fluid properties, geometry of the pore network and the wettability of the pores. The fluid properties are interfacial tensions between fluids, and can be found in the literature. The wettability properties for mercury and nitrogen are also known, such that only the pore properties are unknown in simulations with mercury and nitrogen.

Therefore this process is used to find the pore properties. The curve arising from injection of water into a core plug filled with oil and residual water and the curve arising from injection of gas into a core plug filled with oil and residual water depends on unknown wettability properties and is more complicated to match.

The pore parameters describe the geometry of the network. Maximum and minimum pore radii must be given. The sample of radii are distributed between these two bounds by the power law distribution, $f(r)=r^n$, where n is the power law exponent. The coordination number describes how many pores each node is connected to on average. Since pores in the stone in a reservoir are not necessarily circular, the volume exponent is introduced. The volume in a pore with radius r is $V(r)\propto r^\nu$, where ν is the volume exponent. For pores with circular cross sections the volume exponent will be equal to two. An exponent less than two indicate that the pores are squeezed together and have smaller volume than if they were circular. The seed used to initialize the random number generator is also included amongst the input parameters so that the exact same network can be recreated.

The wettability parameters describe how the different fluids in the network relate to each other. To mimic the state in a reservoir, an ageing option is used. Before the oil took form, the reservoir was water-filled and the pores were water-wet. Then oil streamed into the reservoir and influenced the wettability-state. In the oil-filled pores the wettability is now mixed-wet-large, that is the pores with largest radius are oil-wet, while the pores with smallest radius are water-wet.

To describe the wettability state before ageing, a lower and upper bound for a uniform distribution of the cosines to the wettability angle between oil and water, $\cos(\theta_{ow})$, is given. After ageing the pores have different wettability depending on which phase they were filled with during the ageing. The pores that were water-filled will be described as before ageing, with a lower and upper bound for the cosines, but the values for the bounds are not necessarily the same as earlier. The pores that were oil-filled during ageing have a more complex wettability. They are mixed-wet large, and the minimum radius for oil-wet pores and maximum radius for water-wet pores must be given. A lower and upper bound for cosines for both the oil-wet region and the water-wet region must also be given. What makes it a bit confusing is that the oil-wet region can also contain water wet pores, and the water-wet region can contain oil-wet pores, such that the radii separating them are only radii separating two regions. But since the medium is supposed to be mixed-wet large, the largest pores are mainly oil-wet and the smallest are mainly water-wet.

Films and spreading layers can be present in the network. The presence of films has a large impact on the residual saturations, because a phase that is not connected to

the outlet now can escape through films of the same phase along the pore walls. The parameters in the network describing the films are lower or upper thresholds for oil film around water, oil film or spreading layer around gas, water film around oil, and water film around gas.

All the parameters in the network model are described in Appendix B.

The matching of the parameters can be done both in parallel or sequentially. It seems natural first to determine the geometry of the network by fitting the capillary pressure curve for mercury and nitrogen, before the wettability is estimated by matching the capillary pressure curve for water and oil and the capillary pressure for gas and oil in parallel.

It is possible that some of the parameters do not have an impact on two-phase flow, but will have a large impact when three phases are flowing. These parameters will of course not be estimated correctly when using a scheme that is based on a two-phase anchoring, and tests should therefore be done afterwards to determine the sensitivity of parameters in the presence of three phases.

4.1 Results using EnKF

To be able to evaluate how close the parameters we find by EnKF is to the true ones, we construct a synthetic case. A match to the capillary pressure measurements from a North Sea oil field have already been found by trial and error with the network model, and we choose to use these parameters to create the synthetic case. The same parameters are used to create measurements for the capillary pressure between gas and oil, and water and oil. Since the wettability for mercury and nitrogen is different, some parameters must be modified before creating the measurements for capillary pressure between mercury and nitrogen. The same geometry parameters are used, but the interfacial tension and contact angle between the phases were changed to the value for mercury and nitrogen, and the threshold for films were changed such that there would be films of nitrogen around mercury in all the pores. Also, the ageing option was deactivated.

With this approach we know that there exists a set of parameters that match all three curves perfectly. The output saturations and capillary pressures from these simulations are used as measurements in the following examples. If all the measurements were used, the matching would be very time consuming, and the result would not necessarily be better. Therefor 25 measurements in the case with mercury and nitrogen, 12 measurements in the case with oil and water and the case with gas and oil are used.

Since the wettability for mercury and nitrogen is known, the only unknown parameters in this case are the geometry parameters. The wettability for the other two cases are more complex, and the matching would be easier if the geometry parameters are determined first. Therefore we start with finding the geometry parameters by matching the capillary pressure curve between mercury and nitrogen and then use these in the last two cases.

4.1.1 Capillary pressure between mercury and nitrogen

For each of the five geometry parameters, we select an interval where we assume that the correct parameter value is inside. It is possible to find an estimate of the maximum and minimum pore radii by using the capillary pressures for the lowest and highest saturation of mercury, respectively, and calculate the radii from the Young Laplace equation, Eq. (4.1). For all the parameters we choose the intervals to be so large that we are sure they will contain the correct values, even for real cases where we do not have much information about the properties. We have found that taking the mean of 10 ensembles with 100 members each, is suitable when matching the geometry parameters.

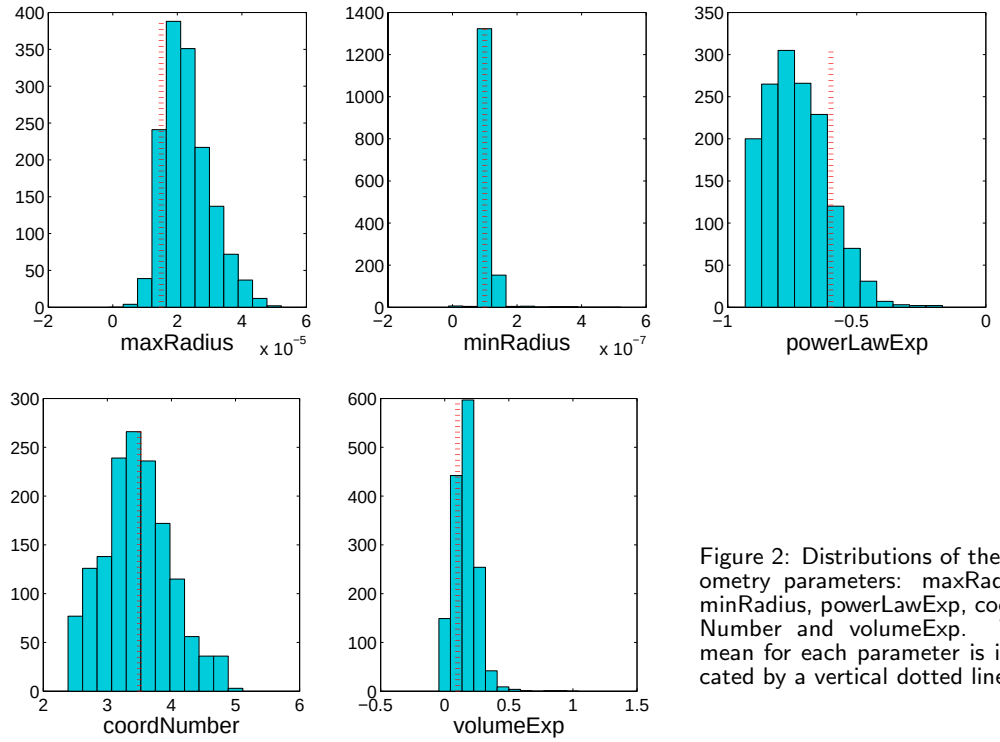

Figure 2: Distributions of the geometry parameters: maxRadius, minRadius, powerLawExp, coordNumber and volumeExp. The mean for each parameter is indicated by a vertical dotted line.

Fig. 2 shows the distributions of each parameter after transforming them back to the uniform distribution in the last time step. The figure contains histograms with the intervals $[\boldsymbol{a},\boldsymbol{b}]$ along the x-axis for each of the parameters. The figure also says something about the uncertainties in the estimated parameter values. If the distribution is wide, it means that parameter values from a large interval can make good matches to the capillary pressure curve. If the distribution is narrow, the interval for the parameter is smaller, and therefore the estimate for the parameter is probably better.

The variance in the distributions of the parameters for different time steps can be seen in Fig. 3.[‡] To also be able to get an impression of the parameters that have very

[‡]Using the law of total variance to construct the variance from a set of ensembles.

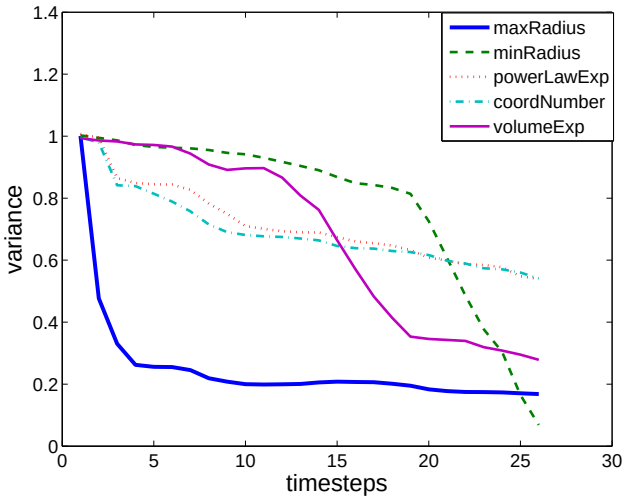

Figure 3: Variance in the distribution of each of the parameters θ_i from section 3, against the number of time steps. (All of these parameters started out in the standard normal distribution with unit variance).

small values, the parameters are transformed to the standard normal distribution. The variances are decreasing as the match becomes better and better. This is shown in Fig. 4. The figure to the left contains the capillary pressure curves from simulations with the parameters in the initial ensemble. The initial ensemble contain parameter values from the whole interval $[a,b]$, and the variation in the parameters is reflected in the variation in the capillary pressure curves. The figure to the right shows the capillary pressure curves from simulations with the last ensemble. Here the curves match the measurements quite well.

Table 1: Table showing the lower and upper bound, true value, estimated value and standard deviation for each of the parameters. See Appendix B for description of the parameters.

Parameter	a	b	true value	est. value	std. dev.
maxRadius	0.1×10^{-5}	5.0×10^{-5}	1.50×10^{-5}	2.30×10^{-5}	0.73×10^{-5}
minRadius	0.1×10^{-7}	5.0×10^{-7}	1.00×10^{-7}	1.07×10^{-7}	0.20×10^{-7}
powerLawExp	-9.0×10^{-1}	-2.0×10^{-1}	-6.00×10^{-1}	-7.32×10^{-1}	1.17×10^{-1}
coordNumber	2.5	5.0	3.50	3.47	0.53
volumeExp	0.0	1.0	1.00×10^{-1}	1.62×10^{-1}	0.92×10^{-1}

Table 1 shows the lower bound a and the upper bound b for each of the parameters, together with the true and the estimated value of the parameters and the standard deviation for the ensemble of parameters in the last time step. The estimated parameters are close to the true ones and the standard deviations are small. If more measurements were used, the standard deviations would be smaller and the estimated parameters closer to the true ones.

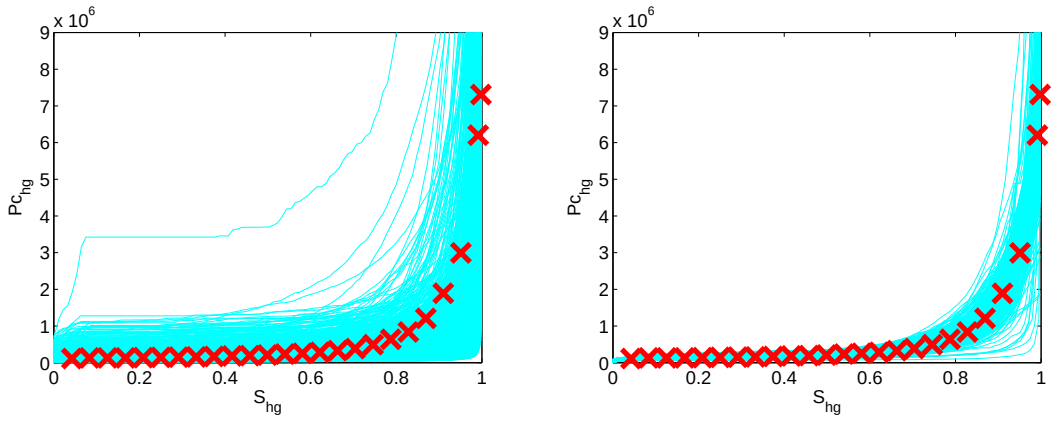

Figure 4: Capillary pressure curves for the parameters in the initial and final ensemble, with the measurements as crosses.

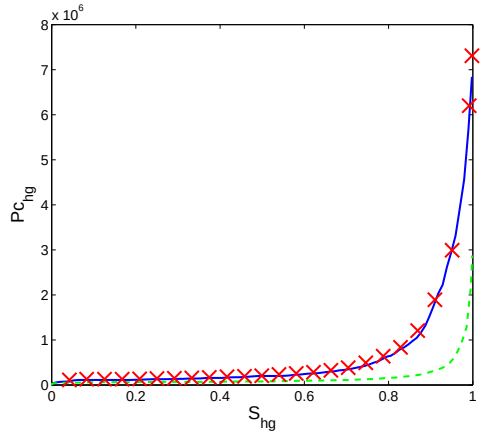

Figure 5: Capillary pressure curve from the mean of the parameters in the final ensemble (solid line), with the measurements as crosses. The curve arising from the mean over the initial ensemble is shown as a dashed line.

The capillary pressure curve arising from the estimated parameters is shown in Fig. 5. The measurements are shown as crosses. The solid curve is made with the estimated parameters, and the dashed curve is made with the mean over the initial ensemble of parameters. The figure shows that all measurements are matched very accurately.

4.1.2 Capillary pressures between oil/water and gas/oil

In the matching of the capillary pressure curves between oil and water, Pc_{ow}, and gas and oil, Pc_{go}, the geometry parameters are locked to the mean values found in the matching of the capillary pressure curve between mercury and nitrogen, Pc_{hg}. We have used 150 members in each of 10 ensembles in the following examples.

The capillary pressure curve between mercury and nitrogen, Pc_{hg}, is defined for all saturations of mercury. For a reservoir with oil and residual water the capillary pressure curve between water and oil is not defined for water saturations less than the residual water saturation and oil saturations less than the residual oil saturation. Similarly, the

capillary pressure curve between gas and oil is not defined for high gas saturations, because of residual water and oil. Near these saturations the amount of fluid possible to inject becomes smaller and smaller, even if the capillary pressure increases a lot, and the capillary pressure curve will have asymptotic behaviour. The asymptotes are important indications of the wettability state in the medium, such that the matching of these are important for finding the wettability parameters. In oil recovery asymptotes tell how much residual oil is left.

First we try to find only five of the wettability parameters: cosLimitFilm_1, cosLimitFilm_2, cosineOFWW2, cosineOFOW2 and rWet1OF. These are the parameters that in our experience are the most sensitive to changes (amongst those we are interested in) and should therefore respond well to filtering. For the rest of the parameters we use the true values. (A description of the parameters is given in Appendix B). For each of the five parameters a lower and upper bound for the parameter values are set. Four of the parameters are cosines, and the intervals for these parameters are all set to $[-1,1]$. The last parameter, rWet1OF, is a radius separating two regions with different wettability, such that the interval for this parameter should cover all pore sizes that are present in the network. If we had some information about the parameter values, the intervals could be smaller.

Table 2: Example with five unknown wettability parameters: Table showing the lower and upper bound, true value, estimated value and standard deviation for each of the parameters. See Appendix B for the description of the parameters.

Parameter	a	b	true value	est. value	std. dev.
cosLimitFilm_1	-1	1	0.84	0.8181	0.0312
cosLimitFilm_2	-1	1	0.98	0.9981	0.0025
cosineOFWW2	-1	1	-0.96	-0.9236	0.0563
cosineOFOW2	-1	1	-0.20	-0.2679	0.0237
rWet1OF	1×10^{-8}	4×10^{-5}	7.00×10^{-6}	8.78×10^{-6}	0.417×10^{-6}

Table 2 shows the interval chosen for each of the parameters, the true value of the parameter, the estimated value of the parameter and the standard deviation for each of the parameters. The estimated mean parameters are quite close to the true ones, and the standard deviations are small compared to the length of the interval $[a,b]$. The capillary pressure curves that the network simulator produces with the estimated mean parameter values are shown in Fig. 6 as solid lines. The measurements are shown as crosses, and the curves made from the initial mean of the parameters are shown as dashed lines. Figs. 6(a) and (c) show the capillary pressure curves between oil and water, while Figs. 6(b) and (d) show the capillary pressure curves between gas and oil.

Because the values of the capillary pressure at the asymptotes are so much larger than for the rest of the measurements, it is not possible to get an impression of how well the measurements between the asymptotes are matched. In Figs. 6(c) and (d) the range is smaller to make it possible to evaluate the match also between the asymptotes. The

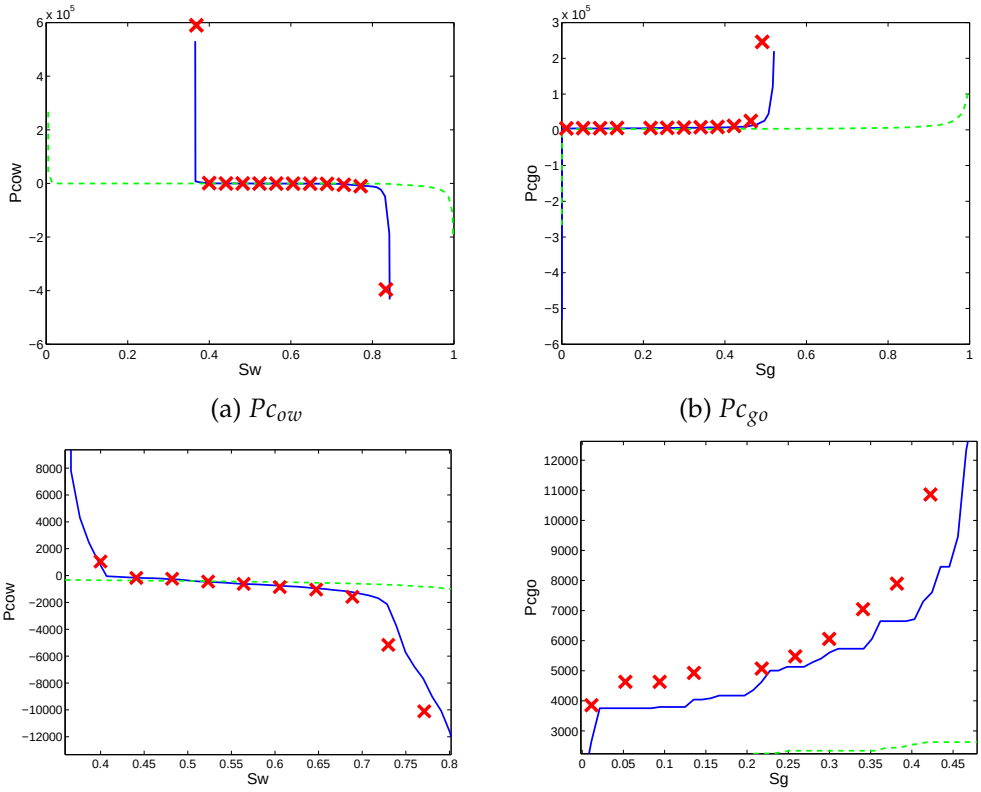

(a) Pc_{ow} (b) Pc_{go}

(c) Pc_{ow} (zoomed in) (d) Pc_{go} (zoomed in)

Figure 6: Example with five unknown wettability parameters: The measurements are shown as crosses, and the capillary pressure curves arising from the initial and last ensembles are shown as dashed and solid lines, respectively.

curves match quite well, especially if they are compared to the initial ones. The asymptote in the capillary pressure curve between gas and oil is not placed exactly where it should be, and from Fig. 6(d) we see that the capillary pressures are too small. This could be attributed to the difference in geometry parameters from the true values.

In general it is harder to match the right asymptote than the left one, because the left asymptote is controlled at every time step. If this should be done for the right one as well, the network model would have to run towards the highest saturation for every time step, and this would make the filtering more time consuming. Note that the conditioning is not a property of the EnKF in general, but stems from the penalty term introduced in Eq. (3.6).

In the following example all fourteen wettability parameters are unknown. As in the previous example, all the cosines are set to be between -1 and 1, and the two parameters separating different wettability regions are set to cover all the radii present in the network.

Table 3 shows the interval, true value, estimated value and standard deviation for

Table 3: Example with fourteen unknown wettability parameters: Table showing the lower and upper bound, true value, estimated value and standard deviation in the ensemble of parameters for each of the parameters.

Parameter	a	b	true value	est. value	std. dev.
cosLimitFilm_0	-1	1	-0.02	0.0371	0.0756
cosLimitFilm_1	-1	1	0.84	0.8133	0.0433
cosLimitFilm_2	-1	1	0.98	0.9369	0.0470
cosLimitFilm_3	-1	1	1.00	0.8975	0.0561
cosineWW1	-1	1	1.00	0.8622	0.0656
cosineWW2	-1	1	0.75	0.7627	0.0501
cosineWF1	-1	1	1.00	0.8885	0.0688
cosineWF2	-1	1	0.80	0.7799	0.0531
cosineOFWW1	-1	1	0.50	0.4871	0.0556
cosineOFWW2	-1	1	-0.96	-0.9168	0.0557
cosineOFOW1	-1	1	0.00	-0.0127	0.0313
cosineOFOW2	-1	1	-0.20	-0.2194	0.0471
rWet1OF	1×10^{-8}	4×10^{-5}	7×10^{-6}	6.540×10^{-6}	0.965×10^{-6}
rWet2OF	1×10^{-8}	4×10^{-5}	7×10^{-6}	7.968×10^{-6}	0.806×10^{-6}

each of the parameters. Some of them match quite well, while others are not close to the true parameters. Also, the standard deviations are larger in this example than in the previous. Fig. 7 shows the capillary pressure curves for the measured parameters, together with the measurements and the initial capillary pressure curves. From Figs. 7(a) and (b) we see that the curves match the measurements quite well even for 14 unknown parameters. The match to the measurements between the asymptotes, shown in Figs. 7(c) and (d), is also similar to the previous example with only 5 unknowns.

Since this problem has more unknowns, the filter was expected to get more problems. It seems like even small variations in the parameters can make a large difference to the capillary pressure curves, especially the asymptotes. Adding more parameters makes the problem even more non-linear and non-Gaussian, increasing the chance that the EnKF will not be able to update the posterior distribution correctly.

Every time the left asymptote has a deviation more than δ, the parameters are updated based on this mismatch and not the mismatch to the present measurement. If this happens often, the measurements between the asymptotes will not be matched very well. In general, if the asymptotes do not match well, this can lead to large changes in the parameters.

The way the network model is built can also be a reason why the parameters do not match. One problem is with the parameters that determine the wettability in pores that are oil-filled during ageing. These pores are divided into two regions with different distributions of contact angles. For one of them the smallest pore radius is given through the parameter rWet1OF, while for the other the largest radius present is given through rWet2OF. It is clear that the filter is not able to separate these two regions from each other. In some cases it seems like they are switched, and the parameters for the first

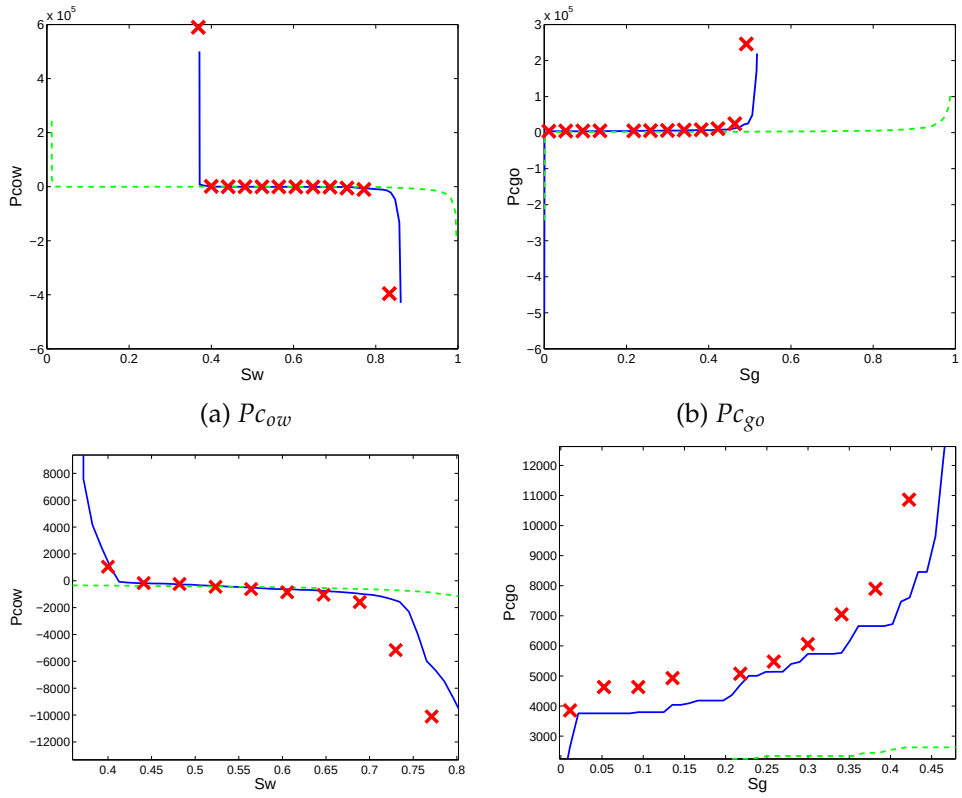

(a) Pc_{ow} (b) Pc_{go}

(c) Pc_{ow} (zoomed in) (d) Pc_{go} (zoomed in)

Figure 7: Example with fourteen unknown wettability parameters: The measurements are crosses, and the capillary pressure curves arising from mean of the initial and final ensembles are shown as dashed and solid lines, respectively.

region match the parameters for the other region instead. This make the matching of the radii separating them, rWet1OF and rWet2OF, difficult as well.

The parameters for films are thresholds of the cosine of the wettability angle. If this threshold is smaller or larger than all the cosines of the wettability angles distributed in the network, the specific value of the threshold has nothing to say.

From earlier testing of the network model we found that different combinations of parameter values can make quite similar capillary pressure curves. Even if parameter values near both boundaries of the interval $[a,b]$ make good matches to the capillary pressure curve, the mean of these does not necessarily make a good match.

A test with smaller intervals $[a,b]$ has also been performed. Of course, the measurements were easier to match in this case. But even when taking into account that the length of the intervals are smaller now, the filter still did a better job in estimating the parameter values relative to the length of the search intervals. When the initial values of the parameters are closer to the true ones, non-unique solutions are avoided, and the filter has an easier job in decreasing the standard deviation for the parameters. If we had information

about the wettability state, this could be used to decrease the interval for some of the parameters.

5 Three-phase surface

Anchoring the three-phase capillary pressures to two-phase gives us a set of values for each parameter, sampled according to the likelihood assigned by the filter for a match with this value. Note that this is a distribution of how well the various values matched the measurements, not necessarily the true distribution of the parameters.

Unless the model is linear, the forward simulation of the mean values will not yield exactly the same result as the mean values indicated by the forward realizations in the ensemble. We thus use the means of the parameter samples as a model of the entire, anchored network, and run simulations with these. To generate values for the three-phase surface, we simulate first an injection of one phase to a certain saturation level before switching to injecting another. This gives us values for different saturation paths, which we in turn afterwards stich together to a surface.

Interpolation must be used to generate a regular surface graph, since the raw paths returned from the network will be somewhat skewed as the injection of for instance gas, will cause drainage of both water and oil simultaneously. If two saturation paths from different injection schemes overlap, we may risk getting slightly inconsistent reading of capillary pressure. These cases are resolved by taking the mean as the representative value, and this does not seem to deteriorate the result.

Not all parts of the three-phase region will be covered, as we are limited to those that can be covered through our injection schemes. For practical purposes these are sufficient, as the points outside of the injections schemes – for instance below residual saturation – are not likely to be encountered in a Darcy-scale simulation anyway.

As imbibition and drainage are two different processes, we need to generate a surface for each of these situations. We have restricted ourselves to one-stage WAG, meaning that only one change of injecting phase takes place. In principle, if more than one change is done, new surfaces should be generated for each combination.

Having three phases means that there are two bilateral capillary pressures; one between oil and water and one between oil and gas. The difference between the pressures in the water and the gas phases can then be inferred from these two.

Therefore, we end up with four graphs for each setup. As can be seen from Fig. 8, the capillary pressure becomes more extreme as one moves from the edges and into the surface, which is consistent with having a lower relative permeability in this area from the presence of another phase.

From these figures, it can also be seen that the amount of residual oil (i.e., oil that cannot be extracted) is decreasing as the gas saturation goes up.

We have confidence that these figures reflect the physical nature of capillary pressure with three phases present [27], thus giving the correct impression of such a surface. Although they are most likely not exact, we hold them to be sufficient approximations.

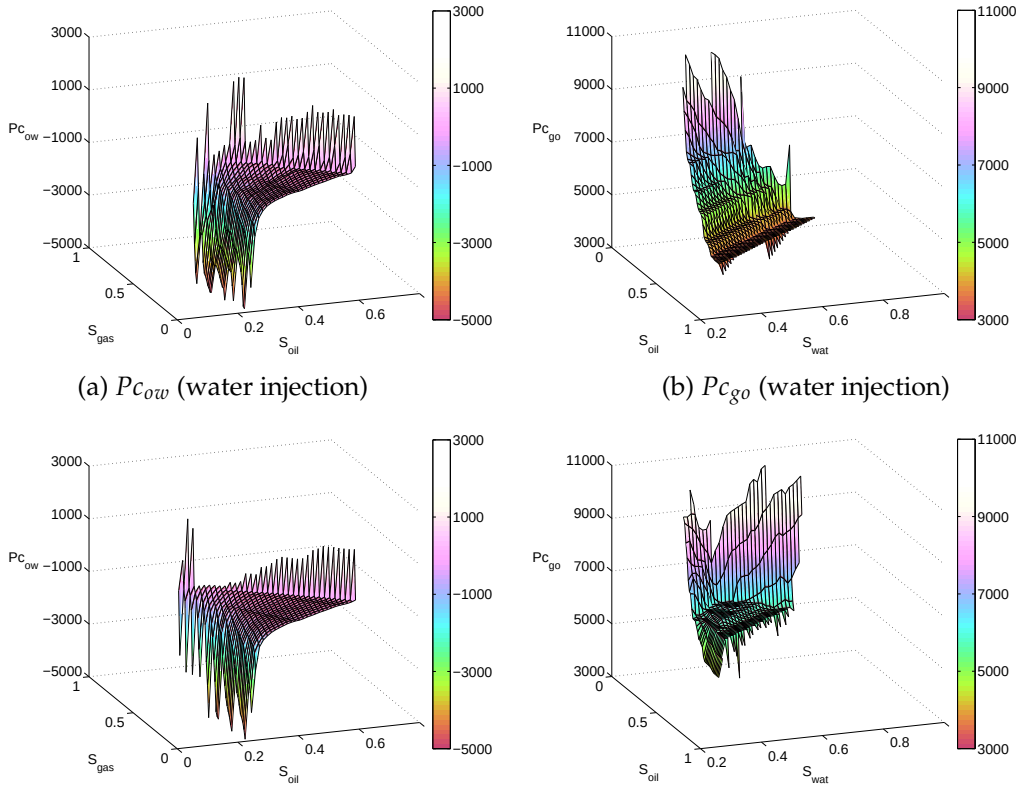

(a) Pc_{ow} (water injection)

(b) Pc_{go} (water injection)

(c) Pc_{ow} (gas injection)

(d) Pc_{go} (gas injection)

Figure 8: Capillary pressure surfaces for oil/water and gas/oil, made with injection of water or gas into a network filled with oil and residual water.

6 Conclusions and further work

In summary, we have identified that the adapted Ensemble Kalman filter may successfully be used to anchor a pore-scale lattice network model to known two-phase data. This inverse problem can give us parameters for running the network model for three-phase flow, resulting in a capillary pressure surface that can be used in continuum-scale reservoir simulations.

The geometry parameters found by matching the capillary pressure between mercury and nitrogen were acceptable. This is also the case when trying to determine a number of unknown wettability parameters by matching the capillary pressure curves from oil and water, and gas and oil flow.

A clear limitation of this method is of course that some parameters can be ambiguous in a two-phase setup, i.e. give the same curves for several combinations, but still have an effect in a three-phase setup and thus result in different surfaces.

The statistics behind the filter assumes a linear model based on Gaussian variables.

The further away from these assumptions the model is, the less reliant the results from the filter will be. Thus, the method is not applicable to every problem.

The accuracy of our results depends mainly on three topics:

- The quality of the two phase data.
- The quality and ability of the network simulator to model the complex physical and chemical mechanisms involved in the dynamical process.
- The quality and generality of our EnKF algorithm to handle the problem studied.

All these represent challenging topics for further research.

An in-house multiphase flow simulator ATHENA [28] has the possibilities of using both two-phase and three-phase capillary pressure and relative permeability tables as input. Several runs have been done to compare production results when using three-phase capillary pressure tables and two-phase capillary pressure tables for an oil/water mixed-wet synthetic reservoir. At the moment three-phase relative permeabilities are not available, so two-phase relative permeabilities have been used in the simulations. We know from theory and experimental works that these parameters are very important for the multiphase flow dynamics. A systematic testing of the sensitivity of three-phase parameters will be performed in later works.

A Nomenclature for EnKF

q			Number of different measurement types,like Pc_{ow}, Pc_{go} and Pc_{hg}
k	$\in[1,q]$		Subscript for measurement type
m			Number of input parameters to the network model
i	$\in[1,m]$		Subscript for parameter number
n			Number of ensemble members
j	$\in[1,n]$		Subscript for ensemble member
ω_k			Number of time steps for measurement type k
t			Superscript for time step
$\boldsymbol{s}$	$\in\mathbb{R}^q$	$=\{s_k\}$	Saturation at time step t for each measurement type k
$\boldsymbol{p}$	$\in\mathbb{R}^q$	$=\{p_k\}$	Measured capillary pressure at time step t for each measurement type k
D	$\in\mathbb{R}^{q\times n}$	$=\{d_{k,j}\}$	Capillary pressure in ensemble member j at time step t for each measurement type k
E	$\in\mathbb{R}^{q\times q}$	$=\{e_{k,k}\}$	Covariance matrix for the error in measurements
$\boldsymbol{\alpha}$	$\in\mathbb{R}^m$	$=\{\alpha_i\}$	Input parameters to network model in their natural domain
f	$\in(\boldsymbol{\alpha},s_k)\rightarrow\psi_k$		Simulator producing a pressure for a given saturation
$\boldsymbol{\psi}$	$\in\mathbb{R}^q$	$=\{\psi_k\}$	Simulation output
$\boldsymbol{s}^L$	$\in\mathbb{R}^q$	$=\{s_k^L\}$	Saturation for the left asymptote in the output from the network model for each measurement type k (only if the curve has a left asymptote)

$\boldsymbol{s}^R$	$\in\mathbb{R}^q$	$=\{s_k^R\}$	Saturation for the right asymptote in the output from the network model for each measurement type k (only if the curve has a right asymptote)
Y	$\in\mathbb{R}^{q\times n}$	$=\{y_{k,j}\}$	Capillary pressure value representing member j
Θ	$\in\mathbb{R}^{m\times n}$	$=\{\theta_{i,j}\}$	Parameter i for member j in Gaussian mapping
g^{-1}	$\in \boldsymbol{u}\to\boldsymbol{\theta}$		Quantile function (i.e. inverse of cumulative) for univariate Gaussian distribution
$\boldsymbol{a}$	$\in\mathbb{R}^m$	$=\{a_i\}$	Lower boundary of search space for each parameter
$\boldsymbol{b}$	$\in\mathbb{R}^m$	$=\{b_i\}$	Upper boundary of search space for each parameter
K	$\in\mathbb{R}^{m\times q}$		Kalman gain
C_{XY}	$\in\mathbb{R}^{m\times q}$		Partial covariance matrix.
$\overline{\Theta}$	$\in\mathbb{R}^{m\times n}$		Mean for each parameter. All columns are equal.
$\overline{Y}$	$\in\mathbb{R}^{q\times n}$		Mean for each simulated pressure. All columns are equal.
δ			The mismatch that we allow for an asymptote
Ξ	$\in\mathbb{R}^{q\times n}$	$=\{\xi_{k,j}\}$	Noise added to pertube the measurements
$\boldsymbol{\sigma}$	$\in\mathbb{R}^q$	$=\{\sigma_k\}$	Standard-deviation for error measurements in graph k at timestep t

B Input parameters to network model

θ_{xy}	contact angle between phases x and y [§]
maxRadius	Maximum pore radius $[m]$ in network
minRadius	Minimum pore radius $[m]$ in network
powerLawExp	Exponent n in power law distribution $f(r)=r^n$ of pore radii r
coordNumber	Average number of connections to pores from each node
volumeExp	Exponent ν in the volume distribution $V(r)\propto r^\nu$
cosLimitFilm_0	Oil films around water will be present for values of $\cos(\theta_{ow})$ lower than this threshold
cosLimitFilm_1	Oil films and spreading layers around gas will be present for value of $\cos(\theta_{go})$ larger than this threshold
cosLimitFilm_2	Water films around oil will be present for values of $\cos(\theta_{ow})$ larger than this threshold
cosLimitFilm_3	Water films around gas will be present for values $\cos(\theta_{gw})$ larger than this threshold
cosineWW1	Maximum value for $\cos(\theta)$ in the uniform distribution of contact angles before ageing, where θ is the contact angle θ_{hgN} between mercury and nitrogen in mercury experiments and θ_{ow} between oil and water in experiments with oil, gas and water

cosineWW2	Minimum value for $\cos(\theta)$ in the uniform distribution of contact angles before ageing, where θ is the contact angle θ_{hgN} between mercury and nitrogen in mercury experiments and θ_{ow} between oil and water in experiments with oil, gas and water
cosineWF1	Maximum value for $\cos(\theta_{ow})$ for water-filled pores after ageing
cosineWF2	Minimum value for $\cos(\theta_{ow})$ for water-filled pores after ageing
rWet1OF	Minimum radius for pores in the part of the network that is most oil-wet. The wettability is mixed-wet large after ageing.
rWet2OF	Maximum radius for pores in the part of the network that is most water-wet. The wettability is mixed-wet large after ageing.
cosineOFWW1	Maximum value for $\cos(\theta_{ow})$ in the fraction of the network that is most water-wet for oil-filled pores after ageing
cosineOFWW2	Minimum value for $\cos(\theta_{ow})$ in the fraction of the network that is most water-wet for oil-filled pores after ageing
cosineOFOW1	Maximum value for $\cos(\theta_{ow})$ in the fraction of the network that is most oil-wet for oil-filled pores after ageing
cosineOFOW2	Minimum value for $\cos(\theta_{ow})$ in the fraction of the network that is most oil-wet for oil-filled pores after ageing

References

[1] A. Skauge and J. Å. Stensen. Review of wag field experience. May 2003. Presented at Oil Recovery - 2003, 1st International Conference and Exhibition Modern Challenges in Oil Recovery, Russia, Moscow, Gubkin University.

[2] T. Holt. Water-alternate-gas injection (wag). In SPOR Monograph: Recent Advances in Improved Oil Recovery Methods for North Sea Sandstone Reservoirs, pages 226–229. 1992. Norwegian Petroleum Directorate.

[3] A. Zolotukhin and J. R. Ursin. Introduction to Petroleum Reservoir Engineering. Høyskoleforlaget, Kristiansand, 2000.

[4] E. I. Dale and A. Skauge. Fluid flow properties of WAG injection processes. Budapest, Hungary, April 2005. The 13^{th} European Symposium on Improved Oil Recovery.

[5] A. Skauge and M. Aarra. Effect of wettability on the oil recovery by WAG. pages 452–459, Moscow, 1993. 7^{th} European Symposium on Improved Oil Recovery.

[6] A. Skauge. Summary of core flood results in connection with WAG evaluation. Number 10 in Wyoming Enchanced Oil Recovery Symposium, University of Wyoming, Laramie, Wyoming, September 1994.

[7] A. Skauge and J. A. Larsen. Three-phase relative permeabilities and trapped gas measurements related to WAG processes. Stavanger, Norway, September 1994. International Symposium of the Society of Core Analysts.

[8] F.J-M. Kalaydjian. Performance and analysis of three-phase capillary pressure curves for drainage and imbibition in porous media. SPE paper 24878. presented at the 1992 SPE Annual Technical Conference and Exhibition, Washington, DC, 4–7 October.

[§]Not to be confused with the θ variable in the EnKF filter

[9] V. Mani and K. K. Mohanty. Pore-level network modeling of three-phase capillary pressure and relative permeability curves. Society of Petroluem Engineers Journal, pages 238–248, September 1998. SPE 50942.
[10] M. I. J. van Dijke, S. R. McDougall, and K. S. Sorbie. Three-phase capillary pressure and relative permeability relationships in mixed-wet systems. Trans. in Porous Media, 44:1–32, 2001.
[11] E. I. Dale and A. Skauge. Features concerning capillary pressure and the effect on two-phase and three-phase flow. In Timing of IOR to Maximise Production Rates and Ultimate Recovery, Cairo, Egypt, 22–24. April 2007. International EAGE - IOR symposium.
[12] J. O. Helland and S. M. Skjæveland. Three-phase capillary pressure correlation for mixed-wet reservoirs. SPE paper 92057, November 2004. presented at the SPE international petroleum conference, Puebla, Mexico.
[13] K. Azis and A. Settari. Petroleum Reservoir Simulation. Applied Science Publishers, 1979.
[14] M. B. Allen III, G. A. Behie, and J. A. Trangenstein. Multiphase Flow in Porous Media, Lecture Notes in Engineering, volume 34. Springer-Verlag, 1988.
[15] J. A. Larsen and A. Skauge. Simulation of the immiscible WAG process using cycle-dependent three-phase relative permeabilities. Society of Petroleum Engineers, 1999. ATC&E, 3-6 October 1999.
[16] A. Kjosavik, J. K. Ringen, and S. M. Skjæveland. Relative permeability correlation for mixed-wet reservoirs. Society of Petroleum Engineers, 2000. SPE 59314.
[17] J. E. Nortvedt, K. Langaas, A. Sylte, H. Urkedal, and A. T. Watson. Estimation of three-phase, relative permeability and capillary pressure functions. In Proceedings of the 5th European Conference on the Mathematics of Oil Recovery, Leoben, Austria, September 1996.
[18] K. S. Sorbie and M. I. J. van Dijke. Fundamentals of three-phase flow in porous media of heterogeneous wettability. Institute of Petroleum Engineering, Heriot-Watt University, Edinburgh, Scotland, September 2004.
[19] G. Evensen. Sequential data assimilation with a nonlinear quasi-geostrophic model using Monte Carlo methods to forecast error statistics. J Geophys Res, 99(C5):10143–10162, 1994.
[20] G. Evensen. The Ensemble Kalman Filter: Theoretical formulation and practical implementation. Ocean Dynamics, pages 343–367, 2003.
[21] G. Evensen. Data Assimilation, The Ensemble Kalman Filter. Springer, 2007.
[22] S. M. Skjæveland, L. M. Siqveland, A. Kjosavik, W. L. Hammervold Thomas, and G.A. Virnovsky. Capillary pressure correlation for mixed-wet reservoirs. SPE, 3(1):60–67, 2000.
[23] J. Nocedal and S. J. Wright. Numerical Optimization, 2nd edition. Springer, 2006.
[24] J. R. Shewchuk. An introduction to the conjugate gradient method without the agonizing pain. `http://www.cs.cmu.edu/~quake-papers/painless-conjugate-gradient.pdf`, August 1994.
[25] G. Nævdal, L. M. Johnsen, S. I. Aanonsen, and E. H. Vefring. Reservoir monitoring and continuous model updating using Ensemble Kalman Filter. SPE Journal 10, pp. 66–74 , March 2005. SPE 84372.
[26] K. Thulin, G. Nævdal, H. J. Skaug, and S. I. Aanonsen. Quantifying monte carlo uncertainty in the ensemble kalman filter. In 10th European Conference on the Mathematics of Oil Recovery (ECMOR), Bergen, Norway, September 2008.
[27] E. I. Dale. Modelling of immiscible WAG with emphasis on the effect of capillary pressure. PhD thesis, University of Bergen, Bergen, Norway, 2008.
[28] I. Garrido, G.E. Fladmark, and M. Espedal. An improved numerical simulator for multiphase flow in porous media. Int J Num Meth Fluids, 44:447–461, 2004.